A ROBUST ATTITUDE MEASURING SYSTEM FOR AGILE SATELLITES

J. Treurnicht W.H. Steyn

University of Stellenbosch, Stellenbosch, South Africa

Abstract: A novel attitude measuring sensor is presented to be used on agile satellites without any angular field of view restrictions. The sensor is based on low-cost, medium resolution attitude vector measurements, obtained from geomagnetic detectors (magnetometers) and coarse sun sensors (solar cells). The vector measurements chosen, have an unrestricted field of view and a reasonably high response bandwidth as required during agile satellite manoeuvres. Low-cost solid state angular rate sensors with moderate to high drift bias are used to propagate the attitude between vector measurements. All sensor outputs are validated by a pre-filtering process to eliminate spurious or faulty sensors, before feeding the data into an extended Kalman filter (EKF). The EKF is used to estimate the attitude quaternion and angular rate sensor (gyroscope) bias vectors. Practical results from a rotating platform is presented to verify the theoretical and simulation performance. This new sensor has direct application in satellite attitude estimation owing to it's robust and good performance.

Keywords: Micro Satellites; Attitude Estimation; Extended Kalman Filter (EKF).

1. INTRODUCTION

The orientation of micro satellites may be robustly determined using two non-coincident vector measurements. A combination of a geomagnetic detector (3-axis magnetometer) and a coarse sun sensor array (solar cells) are a particularly suited pair for a polar or sun synchronous orbit. The combination allows low-cost continuous unrestricted satellite attitude measurements during the important day part of the orbit with reasonable accuracy of better than 1°.

The dynamic performance of an agile satellite may be enhanced using gyroscopes. Unfortunately, these gyroscopes are expensive and power hungry, which limited their use to date on smaller satellites. The availability of MEMS gyroscopes at very low cost (about USD30) makes this option now feasible. The performance and robustness can be extended by using multiples of these gyroscopes per axis.

A novel robust attitude Extended Kalman Filter (EKF) is constructed using an innovation mixing mechanism. This scheme allows the flexible use of multiple sensor vectors without a substantial increase in the complexity of the gain calculation of the EKF.

2. SENSORS

The main attitude sensors consist of:

- Coarse Sun Sensor (CSS), consisting of 6 solar cells, one per satellite facet — see Figure 1. Vector measurements are generated by calculating the current difference from opposite sides. A unit vector is generated from the 3-axis measurement and a confidence flag c_s

is generated based on the measurement size. The current from the solar cell is modulated by the cosine of the incidence angle from normal. Deviations from this ideal response occur when the incidence angle on the panel is small. Correction for the earth Albedo effect, using a earth model, is described in [6].

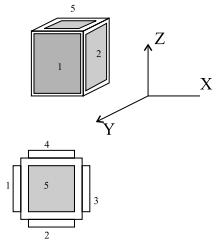

Fig. 1. Coarse Sun Sensor Configuration

- A 3-axis magnetometer (Honeywell HMS2300 or similar). A unit vector is generated from the 3-axis measurement and a confidence flag c_m is generated based on the status (ON, valid communications etc.) and measurement size.
- (Multiple) low-cost MEMS gyros (Analog Devices ADXRS150 or similar), one or more per axis. Depending on the complexity of the temperature and offset compensation, the gyro drift performance can approach 70°/hr.

The formation of the measurement vectors are illustrated in Figure 2.

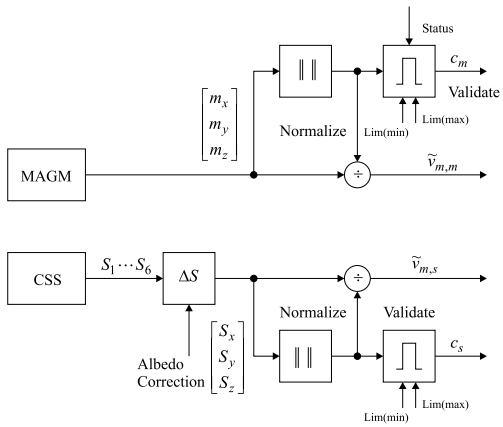

Fig. 2. Forming the Sensor Measurement Vectors

The sun vector can be updated at the desired rate, but the magnetometer measurements will typically be interleaved between magneto-torquer pulses (time-sliced), so a practical magnetometer measurement update period can be 2–10 sec.

3. EKF FORMULATION

Analysis follows that of the Multiplying EKF (MEKF) from [2], [3] and [5].

Let the measurement from the gyro u be related to the actual rate ω, bias rate b and measurement noise η_1

$$u = \omega + b + \eta_1$$

Our best estimate of the rate is then

$$\hat{\omega} = u - \hat{b}$$

The bias rate equation is described by a random walk process

$$\dot{b} = \eta_2$$

Compose the 6-element state vector as consisting of the vector part of the error quaternion $\delta q_1 \ldots \delta q_3$ and the gyro drift-rate bias vector $\delta b_x \ldots \delta b_z$

$$x(t) = \begin{bmatrix} \delta q_1(t) \\ \delta q_2(t) \\ \delta q_3(t) \\ \delta b_x(t) \\ \delta b_y(t) \\ \delta b_z(t) \end{bmatrix}$$

The true attitude quaternion is given by (note the rotated sequence)

$$q = \hat{q} \otimes \delta q$$

where $\otimes$ denotes a quaternion multiplication — see [2], section IV.

The state equation for the system is given by

$$\frac{d}{dt}x(t) = f(x(t), t) + g(x(t), t)w(t)$$

with $w(t)$ = system noise with covariance matrix $Q(t)$.

The state error vector and covariance matrix are defined by

$$\Delta x(t) = x(t) - \hat{x}(t)$$
$$P(t) = \mathcal{E}[\Delta x(t) \Delta x^T(t)]$$

so the state error vector satisfies the differential equation

$$\frac{d}{dt}\Delta x(t) = F(t)\Delta x(t) + G(t)w(t)$$

with

$$F(t) = \frac{\partial}{\partial x} f(x(t), t)|_{\hat{x}(t)}$$
$$G(t) = g(\hat{x}(t), t)$$

The predicted covariance matrix satisfies the differential equation

$$\frac{d}{dt}P(t) = F(t)P(t) + P(t)F^T(t) + G(t)Q(t)G^T(t)$$

For the sixth-order body referenced model, we get

$$F(t) = \left[\begin{array}{c|c} [\omega(t)\times] & -\frac{1}{2} I_{3\times3} \\ \hline 0_{3\times3} & 0_{3\times3} \end{array}\right]$$

$$G(t) = \left[\begin{array}{c|c} -\frac{1}{2} I_{3\times3} & 0_{3\times3} \\ \hline 0_{3\times3} & I_{3\times3} \end{array}\right]$$

We can integrate $F(t)$ numerically to get the discrete state space matrix $\Phi(k)$

$$\Phi(k) = I_{3\times3} + F(k)\delta t + \ldots$$

For a small sample period ($\delta t \ll 1$), we can approximate

$$\Phi(k) \approx \begin{bmatrix} 1 & \omega_z\delta t & -\omega_y\delta t & -0.5\delta t & 0 & 0 \\ -\omega_z\delta t & 1 & \omega_x\delta t & 0 & -0.5\delta t & 0 \\ \omega_y\delta t & -\omega_x\delta t & 1 & 0 & 0 & -0.5\delta t \\ 0 & 0 & 0 & 1 & 0 & 0 \\ 0 & 0 & 0 & 0 & 1 & 0 \\ 0 & 0 & 0 & 0 & 0 & 1 \end{bmatrix}$$

3.1 Innovation

The innovation is determined from the cross-product also used by [4] and [5].

Let the innovation $\mathbf{i}_m(k)$ be given by the cross-product of the measurement $\mathbf{v}_m(k)$ and the reference vector $\hat{\mathbf{v}}_b(k)$ in body coordinates

$$\mathbf{i}_m(k) = \mathbf{v}_m(k) \times \hat{\mathbf{v}}_b(k) = \mathbf{v}_m(k) \times \mathbf{A}(\hat{q})\hat{\mathbf{v}}_r(k)$$

After some manipulation, the measurement sensitivity $H(k)$ becomes

$$H(k) = \left[\, H_a(\hat{\mathbf{v}}_b) \mid 0_{3\times3} \,\right]$$

with

$$H_a(\hat{\mathbf{v}}_b) = 2\begin{bmatrix} \hat{v}_{bz}^2 + \hat{v}_{by}^2 & -\hat{v}_{bx}\hat{v}_{by} & -\hat{v}_{bx}\hat{v}_{bz} \\ -\hat{v}_{by}\hat{v}_{bx} & \hat{v}_{bx}^2 + \hat{v}_{bz}^2 & -\hat{v}_{by}\hat{v}_{bz} \\ -\hat{v}_{bz}\hat{v}_{bx} & -\hat{v}_{bz}\hat{v}_{by} & \hat{v}_{by}^2 + \hat{v}_{bx}^2 \end{bmatrix}$$

3.2 Gain and Covariance Calculation

The covariance update $P^+(k)$ and gain $K(k)$ are calculated by

$$\begin{aligned} K(k) =& P^-(k)H^T(k)\left[H(k)P^-(k)H^T(k) + R(k)\right]^{-1} \\ P^+(k) =& (I - K(k)H(k))P^-(k) \end{aligned}$$

with $Q(k) = \int_0^T G(t)Q(t)G^T(t)\,dt$.

The covariance predictor $P^-(k+1)$ for the EKF is given by

$$P^-(k+1) = \Phi(k)P^+(k)\Phi^T(k) + Q$$

3.3 State Update

- The error quaternion is calculated from the innovation vector $\mathbf{i}_m$ and quaternion gain submatrix K_q

  $$\delta\vec{q}(k) = K_q(k)\,\mathbf{i}_m(k)$$

  and then the error quaternion is normalised

  $$\delta q_4(k) = \sqrt{1 - \|\delta\vec{q}(k)\|}, \quad \delta q(k) = \begin{bmatrix} \delta\vec{q}(k) \\ \delta q_4(k) \end{bmatrix}$$

  The bias vector is calculated from the innovation vector $\mathbf{i}_m$ and bias gain submatrix K_b

  $$\delta b(k) = K_b(k)\,\mathbf{i}_m(k)$$

- The corrected state is now formed from $\hat{x}^+(k) = \begin{bmatrix} \hat{q}^+(k) \\ \hat{b}^+(k) \end{bmatrix}$ with

  $$\hat{q}^+(k) = \delta q(k) \otimes \hat{q}(k)^-$$

  and

  $$\hat{b}^+(k) = \hat{b}(k)^- + \delta b(k)$$

- The predicted state $\hat{x}^-(k+1) = \begin{bmatrix} \hat{q}^- \\ \hat{b}^- \end{bmatrix}(k+1)$ is formed using the quaternion integration from [1]

  $$\hat{q}^-(k+1) = \left[I\cos\frac{\hat{\omega}\delta t}{2} + \frac{\Omega}{\hat{\omega}}\sin\frac{\hat{\omega}\delta t}{2}\right]\hat{q}^+(k),$$

  with $\hat{\omega}(k) = \sqrt{\hat{\omega}_x^2 + \hat{\omega}_y^2 + \hat{\omega}_z^2}$,

  and the bias states are simply propagated as

  $$\hat{b}^-(k+1) = \hat{b}^+(k)$$

3.4 Block diagram

A block diagram combining the above mentioned equations is shown in Figure 3.

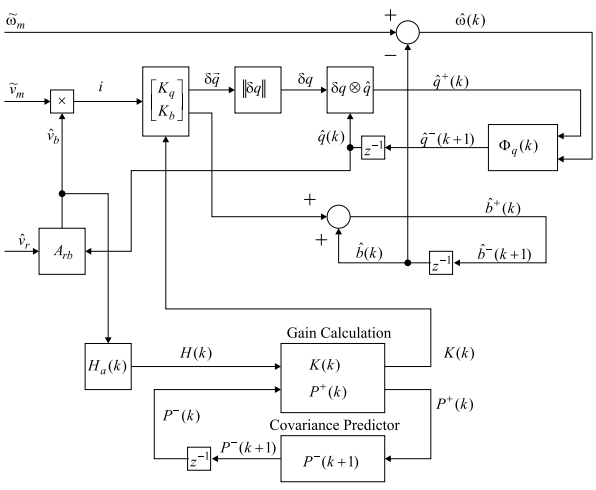

Fig. 3. MEKF Block Diagram

4. SENSOR MIXING

Consider the case in Figure 4 where n sensor measurements (unit vectors) are referred to the body, and n innovation sequences $i_0 \dots i_{n-1}$ are created.

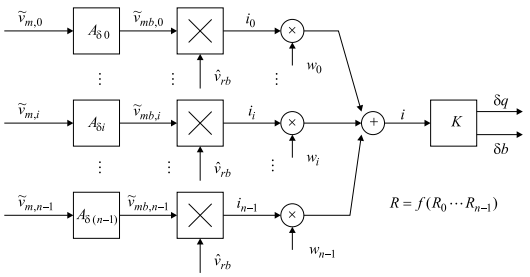

Fig. 4. Innovation based sensor mixing scheme

A number of strategies might be considered for combining the individual innovation sequences into one combined innovation sequence. A weighted scheme was selected

$$\mathbf{i}(k) = \sum_{i=1}^{n} w_i(k)\mathbf{i}_i(k), \quad \sum_{i=1}^{n} w_i(k) = 1$$

The number of vectors in this application are insufficient for implementing a complete fault tolerant scheme. However, it still allows disturbance rejection through the choices of weights. The sensor confidence indicators which checks the total CSS sensor current and magnetic field against a design window, can be used to temporary disable or reduce the effect of a faulty measurement vector.

In the normal case the weights can be based on the known sensor noise covariances R_i. If the two vector measurements are independent, then the weights may then calculated from

$$w_i = \sqrt{R_i}\left[\sum_{j=1}^{n}\sqrt{R_j}\right]^{-1}, \quad R^{-1} = \sum_{j=1}^{n} R_j^{-1}$$

This strategy is simple to implement,and it can accommodate known changes in sensor noise.

For the two-sensor case, we have

$$\begin{aligned} w_1 &= \sqrt{R_1}\left[\sqrt{R_1} + \sqrt{R_2}\right]^{-1}, \\ w_2 &= \sqrt{R_2}\left[\sqrt{R_1} + \sqrt{R_2}\right]^{-1}, \\ R &= R_1 R_2 \left[R_1 + R_2\right]^{-1} \end{aligned}$$

The performance may be further enhanced by modulating the sensor noise covariances at known positions. For example, the geomagnetic measurements close to the poles and the sun sensor measurements at low incidence angles on the solar cells will lead to increased errors for affected vector measurement.

5. PRACTICAL RESULTS

The EKF described was implemented on a demonstrator consisting of rotating base limited in rotation around the Z-axis only. The hardware on this base consisted of 2× yaw measurement ADXL150 MEMS gyros, 4× solar panels and a HMR2300 magnetometer. The measurements were integrated using a Cygnal USB microcontroller at a sample period of 0.1 sec. The attitude EKF was run on a PC in real-time using a C-program.

The reference IGRF and sun vectors are updated using the measurement position latitude-longitude coordinates and local time. No Albedo compensation was performed for these experiments. Compensation for the MEMS gyros were limited to first-order compensation for temperature and offset.

5.1 Measured Performance

The gyro bias estimation performance of the attitude control system, for an arbitary platform attitude rate profile is shown in Figure 5 for the combined sensor innovation strategy.

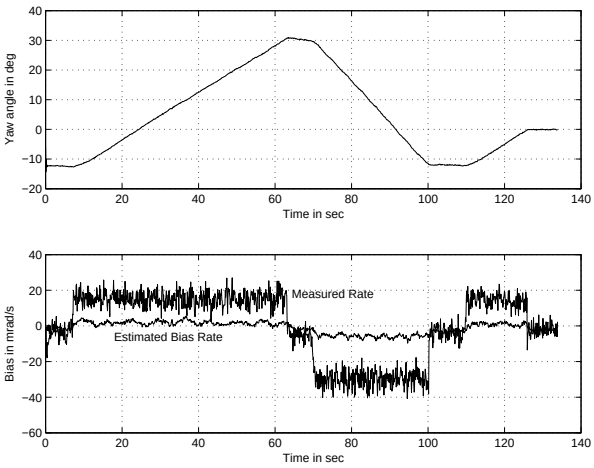

Fig. 5. Typical bias rate estimation

Note that the bias estimate includes effects such as rate calibration errors etc. (the rate scale factor error changes the sign of the bias error in Figure 5).

The typical yaw angle estimation of the attitude control system, with the base rotating at a constant speed about -3 mrad/sec and with the combined sensor innovation strategy, is shown in Figure 6.

6. CONCLUSION

The configuration used in this paper uses the MEKF concepts defined in [2] and [3] with the

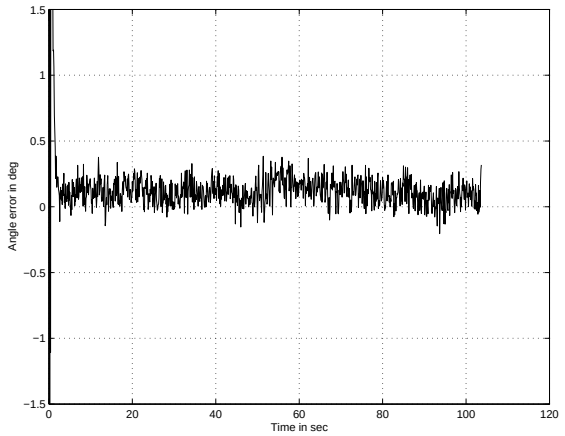

Fig. 6. Typical yaw angle estimation error of the estimated yaw angle relative to the integral of the line-of-sight rate, using both vector measurements and with the platform moving at a constant rate.

cross-product innovation in [4] and [5]. The two sensor vector measurements from the coarse sun sensors and magnetometer similar to [6] is used.

A low-cost gyro is added to extend the tracking performance for an agile satellite, even when the magnetometer data rate is low. Although these gyros are not suitable for the prediction of attitude for longer than a few minutes, their low power and high reliability augments the other sensors to provide a smooth and robust attitude estimate.

A novel method of combining the innovation from the sensors is presented that allows an arbitrary number of sensor measurements to be used simultaneously without a substantial increase in processing. This enables practical on-line EKF gain calculation instead of less accurate fixed-gain banked filters.

REFERENCES

[1] J.R. Wertz (1978), *Spacecraft Attitude Determination and Control*, Kluwer.

[2] E.J. Lefferts, F.L. Markley and M.D. Shuster (1982) *Kalman Filtering for Spacecraft Attitude Estimation*, J Guidance, No. 5, pages 417–429.

[3] F.L. Markley (2003) *Attitude Error Representations for Kalman Filtering*, J Guidance, Control and Dynamics, Vol 26, No.2, pages 311–317.

[4] M.L. Psiaki, F. Martel and P.M. Pal (1990) *Three-Axis Attitude Determination via Kalman Filtering of Magnetometer Data*, J Guidance, Vol 13, No. 3, pages 506–513.

[5] W.H. Steyn (1994), *Full Satellite State Determination from Vector Observations*, WH Steyn, 13th IFAC Symposium, Automatic Control in Aerospace, pages 193–198.

[6] S. Theil, P. Appel and A Schleicher (2003) *Low cost, Good Accuracy - Attitude determination using Magnetometer and simple Sun sensor*, SSC03-XI-7, 17th Annual AIAA/USU Conference on Small Satellites.